MOLECULAR AND CELLULAR BIOLOGY, Aug. 2001, p. 5426–5436 Vol. 21, No. 16
0270-7306/01/$04.00+0 DOI: 10.1128/MCB.21.16.5426–5436.2001

DNA Methylation Is Linked to Deacetylation of Histone H3, but Not H4, on the Imprinted Genes *Snrpn* and *U2af1-rs1*

RICHARD I. GREGORY,[1] TAMZIN E. RANDALL,[2] COLIN A. JOHNSON,[2] SANJEEV KHOSLA,[1]†
IZUHO HATADA,[3] LAURA P. O'NEILL,[2] BRYAN M. TURNER,[2]*
AND ROBERT FEIL[1,4]*

Programme in Developmental Genetics, The Babraham Institute, Cambridge CB2 4AT,[1] and Chromatin and Gene Expression Group, University of Birmingham Medical School, Birmingham B15 2TT,[2] United Kingdom; Gene Research Center, Gunma University, Maebashi 371-8511, Japan[3]; and Institute of Molecular Genetics, CNRS UMR-5535, IRF-24, 34293 Montpellier Cedex 5, France[4]

Received 19 March 2001/Returned for modification 30 April 2001/Accepted 15 May 2001

The relationship between DNA methylation and histone acetylation at the imprinted mouse genes *U2af1-rs1* and *Snrpn* is explored by chromatin immunoprecipitation (ChIP) and resolution of parental alleles using single-strand conformational polymorphisms. The *U2af1-rs1* gene lies within a differentially methylated region (DMR), while *Snrpn* has a 5′ DMR (DMR1) with sequences homologous to the imprinting control center of the Prader-Willi/Angelman region. For both DMR1 of *Snrpn* and the 5′ untranslated region (5′-UTR) and 3′-UTR of *U2af1-rs1*, the methylated and nonexpressed maternal allele was underacetylated, relative to the paternal allele, at all H3 lysines tested (K14, K9, and K18). For H4, underacetylation of the maternal allele was exclusively (*U2af1-rs1*) or predominantly (*Snrpn*) at lysine 5. Essentially the same patterns of differential acetylation were found in embryonic stem (ES) cells, embryo fibroblasts, and adult liver from F1 mice and in ES cells from mice that were dipaternal or dimaternal for *U2af1-rs1*. In contrast, in a region within *Snrpn* that has biallelic methylation in the cells and tissues analyzed, the paternal (expressed) allele showed relatively increased acetylation of H4 but not of H3. The methyl-CpG-binding-domain (MBD) protein MeCP2 was found, by ChIP, to be associated exclusively with the maternal *U2af1-rs1* allele. To ask whether DNA methylation is associated with histone deacetylation, we produced mice with transgene-induced methylation at the paternal allele of *U2af1-rs1*. In these mice, H3 was underacetylated across both the parental *U2af1-rs1* alleles whereas H4 acetylation was unaltered. Collectively, these data are consistent with the hypothesis that CpG methylation leads to deacetylation of histone H3, but not H4, through a process that involves selective binding of MBD proteins.

The differential expression of the maternal and paternal alleles of imprinted genes depends on an epigenetic mark, the imprint, placed on the gene in either the female or male germ line. The nature of such marks remains uncertain, although DNA methylation, specifically methylation of cytosines in CpG dinucleotides, clearly plays a crucial role (36). The maternal and paternal alleles of imprinted loci often have differentially methylated regions (DMRs), with the nonexpressed allele generally, although not always, being more highly methylated (12). As an imprint, CpG methylation has the advantage that transmission from one cell generation to the next is determined by the catalytic properties of DNA methyltransferase 1 (DNMT1). This enzyme preferentially methylates hemimethylated CpGs, thus perpetuating the methylation imprint on daughter strands postreplication (3, 5). However, DNA methylation does not provide a complete explanation for the somatic maintenance of imprints. DMRs must somehow survive the widespread demethylation that occurs following fertilization and during preimplantation stages of development (33, 39, 50). Furthermore, for DMRs that undergo demethylation early in development and are remethylated at later stages (12), methylation cannot be the sole determinant of the epigenetic memory. Finally, there are results to suggest that some imprinted mammalian genes, such as *Mash2* (7, 62), may have an imprinting mechanism that is independent of DNA methylation.

The maintenance of transcriptional states from one cell generation to the next, including imprinted states, may involve the protein components by which DNA is packaged as chromatin (24, 38, 64). The four core histones, H2A, H2B, H3, and H4, despite their extreme conservation through evolution, are all subject to a range of enzyme-catalyzed posttranslational modifications, mostly located in the N-terminal tail domains exposed on the nucleosome surface (25, 37). These modifications provide a rich potential source of epigenetic information. The most widely studied modification, acetylation of selected lysines, has been associated with both short-term and long-term regulation of transcription and transcriptional potential. Changes in acetylation can be transient and local, perhaps confined to just one or two promoter-proximal nucleosomes (9, 34, 45), or spread over chromatin domains of 100 kb or more and linked to progression down specific developmental path-

* Corresponding authors. Mailing address for R. Feil: Institute of Molecular Genetics, CNRS UMR-5535, IRF-24, 1919 Route de Mende, 34293 Montpellier Cedex 5, France. Phone: 33 4 67 61 36 63. Fax: 33 4 67 04 02 03 31. E-mail: feil@igm.cnrs-mop.fr. Mailing address for B. M. Turner: Chromatin and Gene Expression Group, University of Birmingham Medical School, Birmingham B15 2TT, United Kingdom. Phone: 44 121 414 6824. Fax: 44 121 414 6815. E-mail: b.m.turner@bham.ac.uk.

† Present address: Wellcome/CRC Institute of Developmental Biology and Cancer Research, University of Cambridge, Cambridge, United Kingdom.

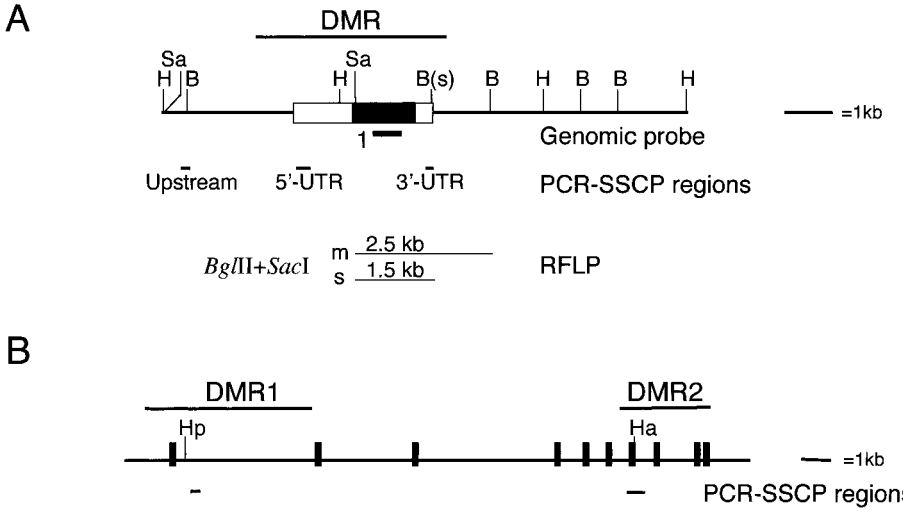

FIG. 1. (A) The imprinted *U2af1-rs1* locus on chromosome 11. The *U2af1-rs1* gene is shown as a box, with its coding part in black. *Hin*dIII (H) and *Sac*I (S) sites, as well as *Bgl*II (B) sites that are polymorphic between *M. musculus* (m) and *M. spretus* (s), are indicated. We determined the DNA sequence of the 11-kb region shown (GenBank accession number AF309654). Sequences analysed by PCR-SSCP are shown as small bars. The line above the gene represents the domain of differential methylation (DMR) and differential nuclease sensitivity (data from references 18, 56, and 57). (B) The imprinted mouse *Snrpn* locus on chromosome 7. Shown are exons 1 to 10 (filled boxes) and the differentially methylated regions DMR1 and DMR2 (horizontal bars above the gene), as defined by Shemer et al. (55). Regions analyzed by PCR-SSCP are indicated, as well as *Hpa*II (Hp) and *Hha*I (Ha) sites that were analyzed for their methylation status.

ways (29, 43, 53). It is also clear that modification of specific lysine residues can be associated with specific transcriptional states (1, 51, 65) and that associations can be stable through the cell cycle and over successive cell generations (8, 15, 63). Recently, other residue-specific histone modifications, such as phosphorylation of H3 serine 10 (10, 11) and methylation of H3 lysines 4 and 9 (47, 60), have been linked to particular functional chromatin states. It is becoming increasingly likely that different tail modifications act in concert to determine the functional properties of chromatin domains (61, 64).

In trying to unravel the role of chromatin features in the establishment and maintenance of imprints, it is important to remember that imprinted genes are subject to the same regulatory constraints as other genes. Imprinted genes often show tissue-specific patterns of expression (18, 46, 48), and changes in chromatin structure or histone acetylation may be contingent on changes in transcriptional status, as well as being components of the epigenetic mark itself. The regulation of imprinted genes is likely to involve a spectrum of interrelated modifications in the DNA, protein, and chromatin structure of imprinted loci. Furthermore, it is quite possible that individual modifications may play greater or lesser roles in the maintenance of the imprint at different stages of development (14, 18, 46, 48, 58, 68).

A long-standing problem in studying the role of chromatin in imprinting mechanisms has been the lack of generally applicable means of distinguishing proteins associated with maternal and paternal alleles. In the present study, we address this problem through a combination of chromatin immunoprecipitation (ChIP), PCR amplification of precipitated material, and electrophoretic detection of single-strand conformational polymorphisms (SSCP). By using cells from hybrid mice, heterozygous for polymorphisms, we have been able to discriminate reliably and quantitatively between the maternal and paternal alleles of the *U2af1-rs1* (chromosome 11) and *Snrpn* (chromosome 7) genes. Both these imprinted genes encode RNA splice factors and are expressed most strongly in the brain and exclusively from the paternal chromosome (20, 21, 27, 28, 35). Previously, we and others reported that the *U2af1-rs1* gene and its direct flanking sequences are methylated, on the maternal chromosome only, in all embryonic and adult tissues analyzed (17, 56). In this domain of differential methylation, chromatin is severalfold more resistant to DNase I on the methylated maternal chromosome than on the unmethylated paternal chromosome (17). Constitutive methylation at the maternal chromosome is also present at the 5′ portion of the *Snrpn* gene, in a region designated DMR1 (Fig. 1). For both the *Snrpn* and *U2af1-rs1* loci, this maternal methylation originates in the oocyte (55, 57). The *Snrpn* DMR1 region is involved in the control of the allelic expression of both *Snrpn* itself and neighboring genes, in a large imprinted chromosomal domain corresponding to the Prader Willi/Angelman region on human chromosome 15q11-q13 (4, 54).

We demonstrate here that differential patterns of histone acetylation distinguish the paternal and maternal alleles at the DMRs of the imprinted *U2af1-rs1* and *Snrpn* genes. We show that DNA methylation is consistently associated with hypoacetylation of histone H3 but not H4. For *U2af1-rs1*, we use transgene-induced methylation of the paternal allele to explore the causal relationship between methylation and histone acetylation and provide in vivo evidence that the allelic CpG methylation at this locus is linked to hypoacetylation of histone H3 but not H4.

MATERIALS AND METHODS

Mice, cell lines, and cell culture. Fetuses that were hybrid for chromosome 11 were produced by crossing a heterozygous male from a newly derived congenic mouse line, SP11, with a C57BL/6 female. SP11 has a *Mus spretus* proximal

chromosome 11 on a C57BL/6 background and was obtained by backcrossing to C57BL/6 for eight generations. Hemizygous males of two transgenic (*U2af1-rs1*) lines (TG8 and TG28) (26) were crossed with C57BL/6 females to generate transgenic and nontransgenic offspring. Primary embryonic fibroblasts were derived from (C57BL/6 × SP11) F_1 fetuses cultured in Dulbecco modified Eagle medium containing 20% fetal calf serum. For the chromatin assays, early-passage (before passage 5) EF1 cells were used that were of a uniform morphology. Embryonic stem (ES) cell lines SF1-1, AG-A, and PR8 were cultured in the absence of feeder cells in ES medium containing 10^3 U of leukemia inhibitory factor (LIF) per ml (13). In all chromatin studies, semiconfluent early-passage (before passage 15) ES cells were used that were morphologically undifferentiated (>90%).

Nuclease sensitivity assays, Southern blotting, and Northern blotting. Nuclei were isolated from tissue or cultured cells and nuclease sensitivity assays were performed as described previously (17). Briefly, purified nuclei were suspended in DNase I or *Msp*I digestion buffer at ~10^7 nuclei/ml. For the DNase I assay, 200-μl aliquots of nucleus suspension were incubated for 10 min at 25°C with increasing amounts of enzyme (Roche). *Msp*I digestions were performed at 37°C in 50 mM Tris-HCl (pH 7.9)–10 mM $MgCl_2$–100 mM NaCl–1 mM dithiothreitol containing 10 U of *Msp*I/μl. Following nuclease digestion and overnight incubation at 50°C with proteinase K, genomic DNA was extracted with phenol-chloroform. After restriction enzyme digestion, electrophoresis through agarose gels and Southern blotting were performed as described previously (17). Northern hybridization was performed as described previously (13), using a 250-bp *Hin*dIII-*Pst*I fragment from the 5′ end of mouse *Gapdh*, a PCR-amplified 499-bp fragment comprising exon 7 of *Snrpn* (see below) and *U2af1-rs1* probe 1 (17).

ChIP, PCR-SSCP, and duplex-PCR. For ChIP assays, purification of nuclei, preparation of chromatin by micrococcal nuclease digestion (to yield fragments of predominantly one to five nucleosomes), and immunoprecipitation with affinity-purified antibodies to acetylated H3 and H4 were all performed as described previously (44). We used the following antisera for ChIP: R252/16 (to H4Ac16), R101/12 (to H4Ac12), R232/8 (to H4Ac8), R41/5 (to H4Ac5), R224/14 (to H3Ac14), and R47/9/18 (to H3Ac9/18) (66, 67). Precipitations to the methyl-Cpg-binding-domain (MBD) protein MeCP2 were performed with a rat polyclonal antibody (Upstate Biotechnology). For PCR-SSCP analysis of precipitated chromatin, 50 ng of each DNA sample was used for PCR (30 to 36 cycles with an annealing temperature of 60°C for all amplifications) in the presence of [α-^{32}P]dCTP (1% of total dCTP). Selected *U2af1-rs1* primers (all defined in the 5′ to 3′ orientation) amplified from three regions: a 192-bp upstream region (forward, ggagtcccaggccaatct; reverse, agcactcagaaggcagag), a 293-bp 5′ untranslated region (5′-UTR) (forward, cgcagatcagacatactgcgg; reverse, tgtggtacggccag cctatg), and a 163-bp 3′-UTR (forward, ctaattcccaaccaagttaca, reverse, aaaacaa catgggaagccag). *Snrpn* primers amplified from two regions: a 228-bp region in DMR1 (forward, aggttgtgactgggatcctg; reverse, gcggcaacagaacttctacc) and a 499-bp region in DMR2 (forward, ttagactggcattgctcgtg; reverse, atgtatctgccccag ccttc). After denaturation of PCR products, DNA was resolved by SSCP gel electrophoresis (23). Briefly, 1 μl of PCR product was added to 10 μl of loading dye (95% formamide, 10 mM NaOH, 0.25% bromophenol blue, 0.25% xylene cyanol). After the samples were heated to 94°C and cooled on ice, 1 to 3 μl of each sample was loaded onto a 0.4-mm thick, 34-cm long nondenaturing polyacrylamide gel (0.5× mutation detection solution [BioWhittaker Molecular Applications Corp.]) and migrated in 0.6× Tris-borate-EDTA (TBE) for 21 to 24 h at 10 V/cm. After being dried, the gels were exposed to X-ray films or analyzed with a phosphorimager (FLA3000; Fuji), after which the relative band intensities were calculated using Quantity-One imaging software (Bio-Rad). For duplex-PCR, 50 ng of template DNA was used (30 cycles), with addition of [α-^{32}P]dCTP (1% of total dCTP) to coamplify from the 293-bp 5′-UTR (see above) and a 161-bp region at α-*Tubulin* (forward, cctgctgggagctctact; reverse, gggttccaggtcta cgaa), or from *Snrpn* DMR1 (see above). PCR products were migrated through nondenaturing polyacrylamide gels. The gels were dried and band intensities were determined as for the SSCP-based analyses. Control duplex-PCR amplifications were conducted with a range of genomic DNA concentrations (2 to 100 ng/30 μl of reaction volume) and different cycle numbers (n = 17 to 36); these yielded identical *U2af1-rs1*/α-*Tubulin* and DMR1/α-*Tubulin* ratios.

RESULTS

***U2af1-rs1* shows paternal-chromosome-specific acetylation of H4 lysine 5 and H3 lysines 14 and 9/18.** Experiments to examine patterns of histone acetylation were carried out on cells from interspecific hybrid mice constructed so that sequence polymorphisms could be used to distinguish maternal and paternal alleles. EF1 fibroblasts were derived from day 14 fetuses that were (C57BL/6 × *M. spretus*)F_1 for proximal chromosome 11 on a homozygous C57BL/6 background. We also analyzed a (C57BL/6 × *M. spretus*)F_1 ES cell line, SF1-1, that we derived previously (13). In both cell lines, digestion at a *Not*I site in the 5′-UTR and at multiple *Hpa*II sites distributed along the gene showed that *U2af1-rs1* is methylated exclusively on the maternal chromosome (data not shown).

To search for parental-chromosome-specific histone acetylation at the *U2af1-rs1* locus, we carried out ChIP on unfixed chromatin fragments prepared from SF1-1 ES cells and EF1 fibroblasts by micrococcal nuclease digestion. The specificity and efficiency of ChIP assays were determined by analyzing proteins extracted from antibody-bound and unbound fractions by sodium dodecyl sulfate-polyacrylamide gel electrophoresis gel and Western blotting (44). In all the ChIP assays presented in this study, protein analysis showed an enrichment of H3 or H4 acetylated at the appropriate lysine residue in the antibody-bound fractions and a parallel depletion in the unbound fractions (data not shown, but see reference 44). In the antibody-bound fractions, the presence of paternal and maternal DNA from different regions of the *U2af1-rs1* locus was determined by PCR amplification followed by electrophoretic detection of SSCP. Crucially for the application of PCR-SSCP to allelic acetylation studies, for all regions analyzed we have found that amplifications from (C57BL/6 × *M. spretus*)F_1 genomic DNA yield equal amounts of C57BL/6- and *M. spretus*-specific fragments on SSCP gels (Fig. 2).

We studied histone acetylation in EF1 primary embryonic fibroblasts at three selected regions within or adjacent to the *U2af1-rs1* locus. Two lie within the domain of maternal-chromosome-specific DNA methylation (5′-UTR and 3′-UTR [Fig. 1A]), and one is upstream of the gene where there is equal methylation on the maternal and paternal chromosomes (17, 56). At the 5′-UTR, levels of histone H4 acetylation at lysines 8, 12, and 16 (H4Ac8, H4Ac12, and H4Ac16) were similar on both the parental chromosomes; i.e., the maternal- and paternal-chromosome-specific bands are of comparable intensities, giving paternal/maternal ratios close to 1. In contrast, with antibodies to H4 acetylated at lysine 5 (H4Ac5), there was a strong enrichment of the paternal *U2af1-rs1* allele in the antibody-bound (acetylated) fraction (Fig. 2A, central panel). Importantly, precipitation with anti-H4Ac5 antibodies gave a parallel depletion of the paternal allele in the unbound (nonacetylated) fraction (Fig. 2A, right panel), For such depletion to occur, a significant proportion of chromatin within the 5′-UTR must carry H4Ac5. Preferential acetylation of the paternal allele was also detected with antibodies to H3 acetylated at lysine 14 (H3Ac14) and lysines 9 and/or 18 (H3Ac9/18) (the antiserum used does not distinguish between H3 acetylated at lysines 9 and 18). Exactly the same enrichment of the paternal allele in H4Ac5, H3Ac14, and H3Ac9/18 was also found at the differentially methylated 3′-UTR (Fig. 2B). In contrast, 2.3 kb upstream of the transcription initiation site and upstream of the region of maternal DNA methylation (Fig. 1A), no significant differences in H3 and H4 acetylation at any lysines were apparent between the parental chromosomes (Fig. 2C). These results are summarized in Table 1.

To determine whether the same paternal-chromosome-specific patterns of H3 and H4 acetylation are present in an adult

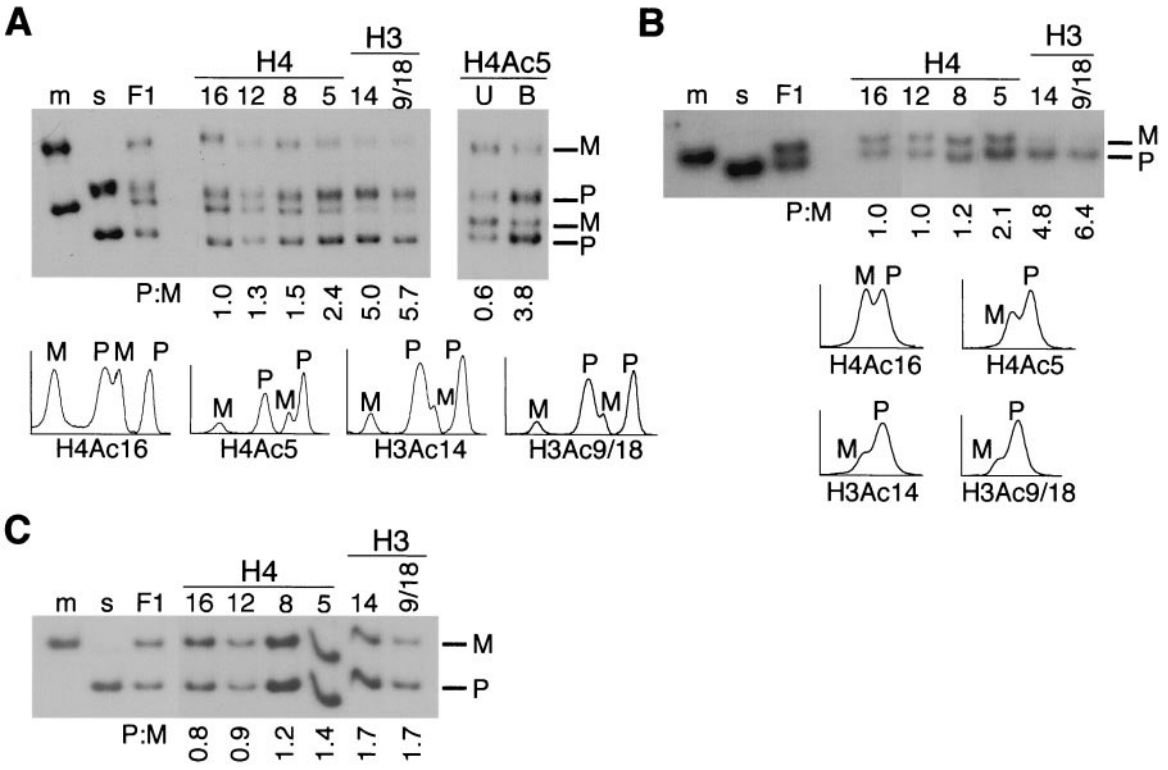

FIG. 2. Paternal H3 and H4 lysine 5 acetylation at *U2af1-rs1* in embryonic fibroblasts. (A) Analysis of acetylation at the 5′-UTR by PCR-SSCP. The first three lanes in the left panel show 5′-UTR PCR products from control liver DNAs, C57BL/6 (m), *M. spretus* (s), and (C57BL/6 × *M. spretus*)F_1 (F1). PCR products derived from the paternal and maternal alleles are indicated by P and M, respectively. Subsequent lanes show PCR products following ChIP with antibodies to H4Ac16, H4Ac12, H4Ac8, H4Ac5, H3Ac14, and H3Ac9/18, respectively. The right panel shows results of an independent precipitation against H4Ac5 that included both the bound (B) and unbound (U) fractions. Paternal/maternal ratios (P:M) are shown beneath each lane. Examples of the lane profiles used for quantification are shown. (B) Acetylation at the 3′-UTR. Control (lanes m, s, and F1) and ChIP samples were as in panel A. Amplification was performed with the 3′-UTR primers. (C) The same control and immunoprecipitated samples were analyzed by PCR-SSCP using primers from the upstream region.

differentiated tissue, we performed ChIP assays on liver chromatin. Livers were dissected from adult mice that were (C57BL/6 × *M. spretus*)F_1 or (*M. spretus* × C57BL/6)F_1 for proximal chromosome 11 (where the *U2af1-rs1* gene is located). Lysine 5 of H4 and lysines 14 and 9/18 of H3 were always acetylated more strongly on the paternal allele in the livers of the two reciprocal genotypes. Indeed, the magnitude of the difference at H4Ac5 between the maternal and paternal chromosomes was greater than in the EF1 fibroblasts, with a more than 10-fold enrichment of the signal on the paternal chromosome (Table 1). These experiments formally prove that the allelic acetylation differences we observed are parent-of-origin dependent and not strain dependent.

Allelic H4 lysine 5 and H3 acetylation patterns at *U2af1-rs1* are established before differentiation. To determine whether the paternal-chromosome-specific H3 and H4 acetylation at *U2af1-rs1* is established before differentiation of the embryonic lineages, ChIP assays were performed on chromatin from undifferentiated ES cells. These are approximately equivalent to the pluripotent inner-cell-mass cells of blastocysts. At both the 5′-UTR and the 3′-UTR, H4 lysine 5, but not lysines 8, 12, and 16, was acetylated predominantly on the paternal chromosome, while for H3, there was preferential paternal acetylation at lysines 14 and 9/18 (Fig. 3A and B, and Table 1). Thus, the characteristic differences in acetylation of paternal and maternal *U2af1-rs1* chromatin are established prior to differentiation. In the region 2.3 kb upstream of the gene, equal levels of H3 and H4 acetylation were detected on maternal and paternal chromosomes (Table 1).

Analysis of *U2af1-rs1* mRNA levels on Northern blots showed that expression was severalfold higher in fibroblasts (sevenfold) and liver (fourfold) than in ES cells (Fig. 3C). In all three cell types, expression was exclusively from the paternal allele (reference 17 and data not shown). Despite these differences in expression level, the relative levels of H3 and H4 acetylation on the paternal and maternal *U2af1-rs1* alleles (the paternal/maternal acetylation ratio) were generally similar in the three different cell types (Table 1). Acetylation levels did not reflect the level of *U2af1-rs1* expression from the paternal allele.

Paternal-allele-specific H3 and H4 acetylation is also found at the maternally methylated imprinting control center of the *Snrpn* gene. The 5′ portion of the *Snrpn* gene on mouse chromosome 7 has a well-characterized DMR (DMR1; Fig. 1B) with maternal DNA methylation that is established in the female germ line and maintained throughout development (55). DMR1 corresponds to the "imprinting-control center" that is involved in the regulation of allele-specific gene expression at

TABLE 1. Summary of PCR-SSCP data for *U2af1-rs1*, presented as the range of paternal/maternal ratios based on multiple ChIP assays[a]

Cell type and histone isoform	Paternal/maternal ratio for:		
	Upstream	5′-UTR	3′-UTR
SF1-1 ES cells			
H4Ac16	1.3–1.8	0.9–1.4	1.5–1.8
H4Ac12	1.3	0.6–0.8	1.3–1.8
H4Ac8	1.3	0.6–0.8	1.4–1.6
H4Ac5	1.3	2.9–3.0	2.7–2.8
H3Ac14	1.0–1.6	3.8–5.5	3.2–5.0
H3Ac9/18	1.5–1.7	4.4–6.4	4.5
EF1 fibroblasts			
H4Ac16	0.8–1.1	1.0–1.4	1.0
H4Ac12	0.9–1.1	1.3–1.5	1.0–1.5
H4Ac8	1.2	1.5–1.7	1.2–1.6
H4Ac5	1.2–1.4	2.4–3.8	2.1–2.4
H3Ac14	1.7–1.9	5.7–>10	4.8–>10
H3Ac9/18	1.7	5.0–>10	6.4–>10
$(C57BL/6 \times SP11)F_1$ and $(SP11 \times C57BL/6)F_1$ liver			
H4Ac16	0.9–1.0	1.5	1.3
H4Ac5	1.4–1.5	>10	2.1–2.6
H3Ac14	1.5–1.7	5.6–6.4	4.3–6.3
H3Ac9/18	1.0	>10	3.1–4.2

[a] *Snrpn* data are based on a single series of experiments (Fig. 4 and 5) and do not appear in the table.

the Prader-Willi/Angelman domain on human chromosome 15q11-q13 (4, 54). We have used the ChIP-SSCP approach with chromatin from hybrid ES cells and adult tissue and PCR-SSCP to determine whether maternal methylation correlates with H3 and H4 hypoacetylation at this imprinting-control center.

In early-passage SF1-1 ES cells, with unaltered maternal methylation at the *Snrpn* DMR1 (Fig. 4 and data not shown), H3 acetylation at lysines 14 and 9/18 was detected on the paternal (unmethylated, expressed) chromosome only. For H4, there was a generally higher level of acetylation on the paternal chromosome than on the maternal (methylated, repressed) chromosome, with paternal/maternal ratios ranging from 1.8 to 4.7 (Fig. 4). As with *U2af1-rs1*, the strongest allelic difference in H4 acetylation was at lysine 5. These allelic differences were not confined to ES cells. Essentially the same pattern of allele-specific H3 and H4 acetylation was found when chromatin from adult mouse liver was subjected to the same type of analysis (data not shown). By Northern analysis, we established that *Snrpn* expression was relatively high in the SF1-1 ES cells whereas little expression was detected in adult liver (Fig. 3C). Thus, the paternal/maternal acetylation differences at the DMR1 do not reflect the level of (paternal) *Snrpn* expression.

Paternal-allele-specific acetylation of H4, but not H3, in the 3′ region of *Snrpn*. *Snrpn* has a second region (DMR2; Fig. 1B) that has been reported to be methylated more highly on the expressed paternal than on the repressed maternal allele in some adult tissues (55). We did not find evidence for paternal-allele-specific DNA methylation at DMR2 in undifferentiated SF1-1 ES cells. We analyzed the methylation status of a single, methylation-sensitive *Hha*I restriction site in exon 7 of *Snrpn* (Fig. 1A). In the brain, this site is prefentially methylated on the paternal allele (55). In contrast, we found that in the SF1-1 cells and the liver, this site was methylated on both parental alleles (Fig. 5B). Methylation at this *Hha*I site and two directly flanking *Hha*I sites was also analyzed in the androgenetic and parthenogenetic ES cell lines, using a Southern hybridization approach. This confirmed that in ES cells, this region is highly methylated on both parental chromosomes (data not shown). In SF1-1 ES cells, the relative levels of H3Ac14 and H3Ac9/18 on DMR2 were equal on the maternal and paternal chromosomes (Fig. 5). In contrast, for H4 there was differential acetylation of this region, with much higher acetylation levels on the expressed paternal than on the repressed maternal chromosome. We also found comparable levels of maternal and paternal DMR2 methylation in the liver (Fig. 5A) and did not detect allelic differences in H3 acetylation. However, as in ES cells, we found paternal H4 acetylation at all lysines analyzed (data not shown).

Acetylation patterns in androgenetic and parthenogenetic ES cells. The high levels of acetylation on the paternal relative to the maternal *U2af1-rs1* and *Snrpn* alleles, as measured by ChIP-SSCP, could be due to hyperacetylation (compared to nonimprinted genes) of the paternal allele, to hypoacetylation of the maternal allele, or to a combination of the two. To address this, we immunoprecipitated chromatin from early-passage androgenetic (dipaternal) and parthenogenetic (dimaternal) ES cell lines. In the lines selected, *U2af1-rs1* was almost completely methylated (parthenogenetic line PR8 [13]) or unmethylated (androgenetic line AG-A [17]) at the passages used. DNA samples were extracted from antibody-bound fractions and used as templates to coamplify PCR fragments from *U2af1-rs1* and α-*Tubulin*, a ubiquitously expressed gene previously shown to have moderate levels of acetylation typical of euchromatic genes (31; L. P. O'Neill, unpublished results). PCR products were size fractionated through polyacrylamide gels, and their relative abundance was determined (Fig. 6A). For histone H3, relatively high levels of acetylation at all lysines tested were detected in the AG-A cells (2- to 3-fold higher levels than α-*Tubulin*) and relatively low levels were detected in the PR8 cells (0.3- to 0.5-fold lower levels than α-*Tubulin*). In contrast, with only one exception, H4 acetylation at all lysines was similar on the *U2af1-rs1* and α-*Tubulin* genes in both the AG-A and PR8 cells. The one exception was that in PR8 (dimaternal) cells, H4Ac5 at *U2af1-rs1* was relatively low, at about 0.3 times the value for α-*Tubulin* (Fig. 6A). These findings are consistent with the relative levels of acetylation of the maternal and paternal *U2af1-rs1* alleles measured by PCR-SSCP in SF1-1 and EF1 cells. They also suggest that whereas H3 acetylation is both increased on the paternal *U2af1-rs1* allele and decreased on the maternal allele, the maternal-paternal difference in H4Ac5 is due primarily, and perhaps exclusively, to a reduction in the level of H4Ac5 on the maternal allele.

We also tested the levels of H3 and H4 acetylation at *Snrpn* in the androgenetic and parthenogenetic ES cell lines. As expected, the DMR1 was methylated in the parthenogenetic PR8 cells and unmethylated in the androgenetic AG-A cells (data not shown). In the AG-A cells, DMR1 showed relatively high levels of acetylation, compared to the α-*Tubulin* gene, at all H3 and H4 lysine residues tested, with H3 giving the highest values (Fig. 6B). In PR8 cells, the levels of acetylation at lysine 5 of H4 and at lysines 14 and 9/18 of H3 were substantially lower at

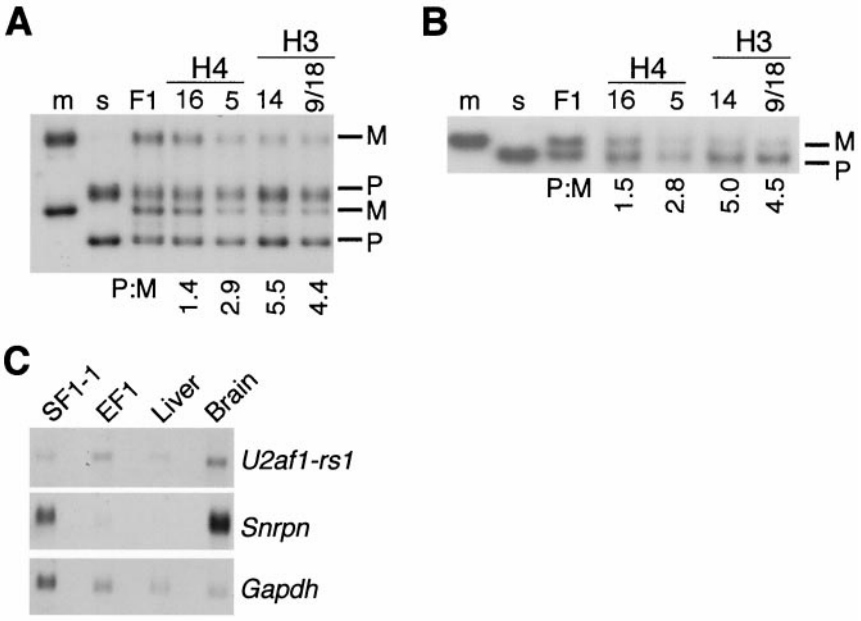

FIG. 3. Paternal H3 and H4 lysine 5 acetylation at *U2af1-rs1* in ES cells. (A) Acetylation at the 5′-UTR. ChIP was performed on chromatin extracted from SF1-1 cells. PCR and SSCP analysis were performed as for Fig. 2A. (B) Acetylation at the 3′-UTR. DNA samples derived from the same ChIPs as for the 5′-UTR were used for PCR amplification with primers from the 3′-UTR (as in Fig. 2B). (C) Northern analysis of *U2af1-rs1* and *Snrpn* expression. Total RNAs from SF1-1 and EF1 cells and from adult (C57BL/6 × *M. spretus*) F_1 liver and brain were hybridized with *U2af1-rs1* probe 1, an exon 7 probe of *Snrpn*, and a mouse *Gapdh* probe. Optical density measurements established that the intensity of the *U2af1-rs1* signal, relative to that of *Gapdh*, was 0.1 (SF1-1), 0.7 (EF1), 0.4 (liver), and 2.4 (brain).

DMR1 than at α-*Tubulin*. In contrast, acetylation of lysines 16, 12, and 8 of H4 was only slightly lower at DMR1 than at α-*Tubulin* (Fig. 6B). These findings are consistent with the relative levels of acetylation of the maternal and paternal DMR1 alleles that we measured by PCR-SSCP in the SF1-1 ES cells and similar to the levels of H3 and H4 acetylation at *U2af1-rs1* in AG-A and PR8 cells (see above). In fact, the only significant difference between the two genes, in terms of the levels of H3 and H4 acetylation on the maternal and paternal alleles, is that whereas the *Snrpn* DMR1 region shows differential acetylation of all H4 lysines (with lysine 5 showing the greatest difference), for *U2af1-rs1* the difference is confined to H4 lysine 5.

Transgene-induced CpG methylation on the paternal *U2af1-rs1* allele correlates with deacetylation of histone H3. To investigate whether CpG methylation affects the acetylation status of H3 and H4, we analyzed mice that had acquired a *U2af1-rs1* methylation imprint in both the female and the male germ lines. We have previously reported that *U2af1-rs1* methylation can be affected by the presence, in the testis, of multiple copies of a transgene construct comprising the entire *U2af1-rs1* gene plus 2.9 kb of upstream sequences and 2 kb of downstream sequences (26). We showed that offspring (even nontransgenic ones) of hemizygous transgenic males acquired full methylation on the normally unmethylated paternal allele at a low frequency. As on the maternal chromosome (57), this

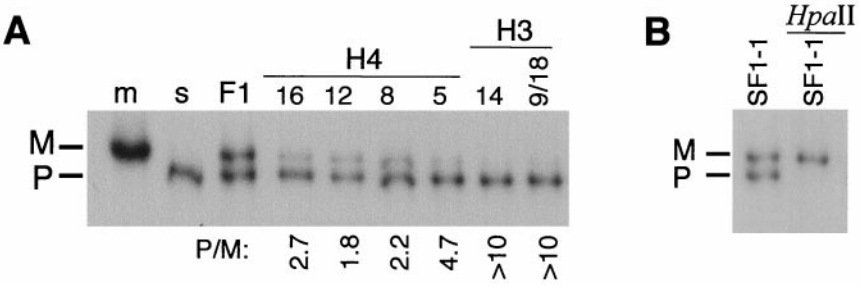

FIG. 4. Differential H3 and H4 acetylation at DMR1 of *Snrpn*. (A) Analysis of DMR1 acetylation in SF1-1 ES cells. Lanes m, s, and F1 in the left panel show DMR1 PCR products from control liver DNAs [C57BL/6, *M. spretus*, and (C57BL/6 × *M. spretus*) F_1, respectively]. Subsequent lanes show PCR products following ChIP on chromatin from SF1-1 ES cells with antibodies to H4Ac16, H4Ac12, H4Ac8, H4Ac5, H3Ac14, and H3Ac9/18. Measured paternal/maternal ratios (P:M) are shown underneath each lane. (B) PCR-SSCP-based analysis of DNA methylation at DMR1. SF1-1 ES cell DNA was PCR amplified with the DMR1 primers and migrated on an SSCP gel (left lane). The right lane corresponds to the same DNA sample, digested with the methylation-sensitive endonuclease *Hpa*II prior to PCR amplification. Maternal methylation was confirmed by Southern hybridization (data not shown).

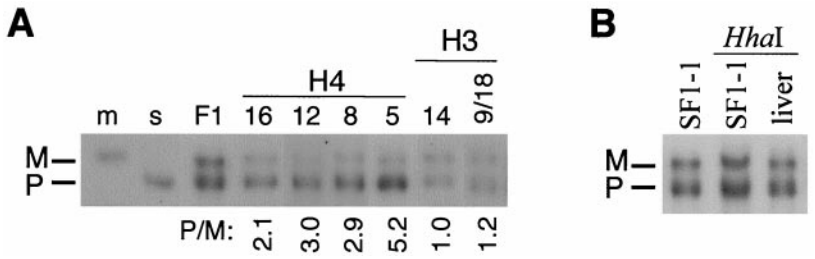

FIG. 5. Differential H4, but not H3, acetylation at the DMR2 of *Snrpn*. (A) Analysis of acetylation at the DMR2 in SF1-1 ES cells. Lanes m, s, and F1 in the left panel show DMR2 PCR products from control liver DNAs [C57BL/6, *M. spretus*, and (C57BL/6 × *M. spretus*)F_1, respectively]. Subsequent lanes show PCR products (DMR2 primers) following ChIP with antibodies to H4Ac16, H4Ac12, H4Ac8, H4Ac5, H3Ac14, and H3Ac9/18 (the same ChIP series as in Fig. 4A). Paternal/maternal ratios (P:M) are shown underneath each lane. (B) PCR-SSCP-based analysis of DNA methylation in the DMR2 region. In the left lane, genomic DNA from SF1-1 ES cells was PCR amplified using the DMR2 primers and then separated by SSCP. The middle lane shows the same DNA digested with the methylation-sensitive endonuclease *Hha*I prior to amplification. The right lane shows the PCR product amplified from *Hha*I-digested (C67BL/6 × *M. spretus*)F_1 liver DNA.

paternal methylation was found to spread throughout the locus during early development. This was observed in two independent transgenic lines, TG8 and TG28, both of which had 20 to 30 copies of the transgene (26). In the present study, we crossed hemizygous males of these two transgenic lines with C57BL/6 females. From each cross we selected one nontransgenic offspring that had methylation on the paternal *U2af1-rs1* allele in addition to the maternal gene. In these two offspring (designated TG8-BF3-11 and TG28-BF2-46), the *Not*I restriction site at the 5′-UTR was fully methylated in liver (Fig. 7A), as were all 24 *Hpa*II sites across the gene (data not shown). These animals also showed no expression of *U2af1-rs1* (data not shown, but see reference 26). To analyze the levels of histone acetylation in these two animals, we purified liver nuclei and performed ChIP assays on chromatin. To determine the levels of *U2af1-rs1* acetylation relative to those at the α-*Tubulin* gene, we performed duplex-PCR amplification on DNA from immunoprecipitated fractions. The results for TG28-BF2-46 are shown in Fig. 7B. In comparison to a control (C57BL/6 × *M. spretus*)F_1 liver, TG28-BF2-46 revealed strongly reduced levels of H3 acetylation (lysines 14 and 9/18) on *U2af1-rs1*. In contrast, the levels of H4 acetylation (lysines 5 and 16) were the same in TG28-BF2-46 and the F_1 control. These results demonstrate that histone H3, but not histone H4, is hypoacetylated on both the methylated parental chromosomes.

MBD proteins associate with the maternal allele of *U2af1-rs1*. One mechanism by which the maternal DNA methylation at *U2af1-rs1* could confer the observed maternal hypoacetylation at H3 is the association of specific methyl-CpG-binding-domain (MBD) proteins and subsequent recruitment of histone deacetylases (32, 40). In support of this possibility, we found that across the *U2af1-rs1* gene the maternal chromosome was highly resistant to the methylation-insensitive restriction endonuclease *Msp*I in purified nuclei. This was observed in the SF1-1 ES cells (Fig. 8A) and also in adult liver cells in a previous study (17). Four *Msp*I sites within a polymorphic *Bgl*II-*Sac*I fragment (Fig. 1A) were highly sensitivity to *Msp*I on most of the paternal chromosomes, whereas these sites were *Msp*I resistant on most of the maternal chromosomes (Fig. 8A). Similar results were obtained when 24 *Msp*I sites distributed along the entire *U2af1-rs1* locus were studied (data not shown).

To test directly for the allelic association of MBD proteins, we precipitated chromatin from (C57BL/6 × SP11)F_1 liver with an antiserum against the MBD protein MeCP2. Allele-specific analysis of immunoprecipitated chromatin at the 5′ UTR of *U2af1-rs1* showed that MeCP2 was associated almost exclusively with the maternal (methylated) allele (Fig. 8B).

DISCUSSION

Patterns of H3 and H4 acetylation on imprinted genes. In the present report, we describe how a combination of ChIP, PCR amplification, and detection of SSCP can be used to define patterns of histone acetylation along the maternal and paternal alleles of the imprinted genes *Snrpn* and *U2af1-rs1*. At the *U2af1-rs1* gene, in ES cells, fibroblasts, and liver cells, we found that (i) H3 is more highly acetylated at lysines 14 and 9/18 on the paternal allele than on the maternal allele; (ii) H4 is more highly acetylated at lysine 5 on the paternal allele than on the maternal allele; and (iii) H4 acetylation at lysines 8, 12, and 16 is essentially the same on the maternal and paternal alleles. We emphasize that these allelic differences have been consistent through multiple experiments with different cells and tissues and when using different antisera. They also occur at opposite ends of the differentially methylated region of *U2af1-rs1*, namely, the 5′-UTR and the 3′-UTR. Acetylation differences are not present in a region 2.3 kb upstream of the gene that has equal DNA methylation on both the parental chromosomes.

The differentially methylated CpG island DMR1 in the 5′ region of the mouse *Snrpn* gene (54) is homologous to the imprinting control center of the Prader-Willi/Angelman domain on human chromosome 15q11-q13 (4, 54). For DMR1, allele-specific acetylation studies revealed high levels of H3 and H4 acetylation on the paternal (unmethylated, expressed) allele relative to the maternal (methylated, repressed) allele, both in ES cells and in adult liver cells. As with *U2af1-rs1*, differential H3 acetylation was apparent at all lysines tested (lysines 14, 9, and 18) whereas for H4, the differential acetylation was most pronounced for lysine 5. However, unlike *U2af1-rs1*, there was also a small but consistent elevation of H4 acetylation at lysines 8, 12, and 16 on the paternal allele. The *Snrpn* gene contains a DNA element within its coding region that is methylated more highly on the paternal chromosome

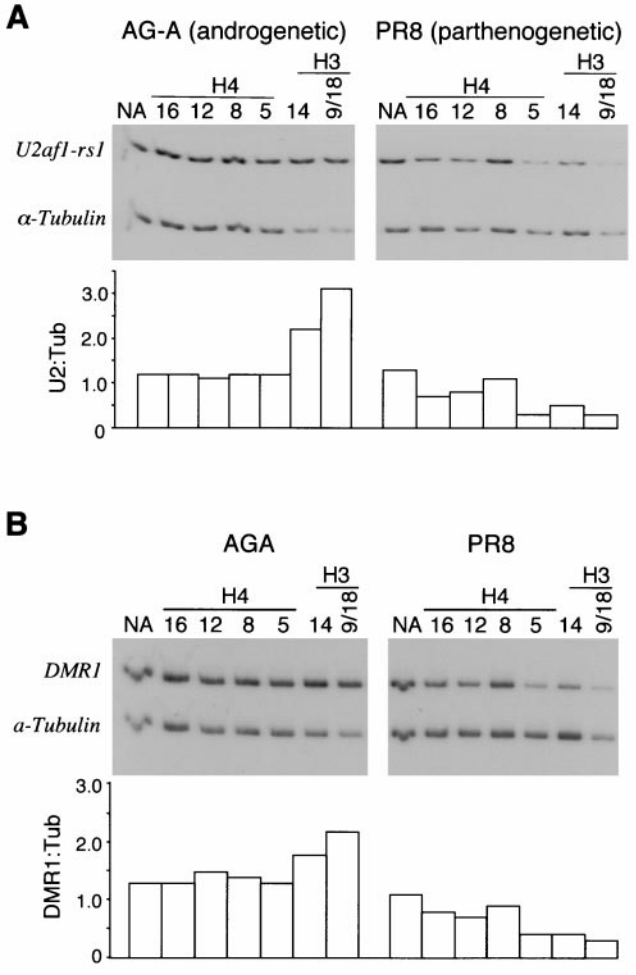

FIG. 6. Analysis of H3 and H4 acetylation in monoparental ES cells. (A) Levels of *U2af1-rs1* acetylation. ChIP assays were performed on AG-A (androgenetic) and PR8 (parthenogenetic) ES cells. DNA, extracted from the immunoprecipitated fractions was used to coamplify with primers from *U2af1-rs1* (5′ UTR) and *a-Tubulin*. Ratios between the *U2af1-rs1*- and *a-Tubulin*-amplified fragments (U2:Tub) are plotted underneath the gels. The first lanes indicate amplification from input chromatin to which no antibody (NA) was added. (B) Levels of *Snrpn* DMR1 acetylation. ChIP was performed on chromatin from AG-A and PR8 ES cells. DNA extracted from the immunoprecipitated fractions coamplified with primers from the DMR1 and *a-Tubulin*. Ratios between DMR1 and *a-Tubulin* products (DMR1:Tub) are plotted underneath the gels. NA indicates amplification from no-antibody control samples.

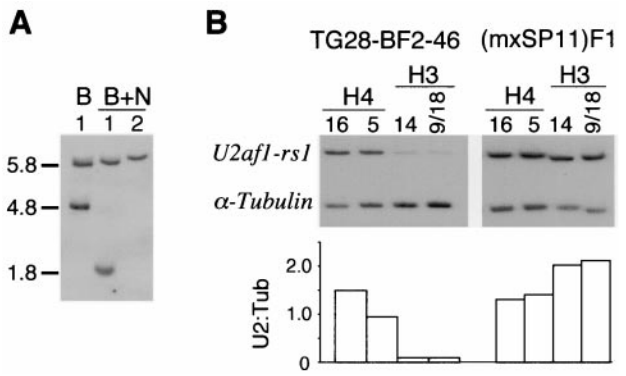

FIG. 7. CpG methylation is linked to H3 underacetylation at *U2af1-rs1*. (A) Genomic DNAs were digested with *Bgl*II (B) or *Bgl*II-*Not*I (B+N) and analyzed by Southern hybridization with probe 1. Lanes 1 correspond to (C57BL/6 × SP11)F_1 liver DNA, lane 2 corresponds to liver DNA from mouse TG28-BF2-46. (B) ChIP assays were performed on TG28-BF2-46 liver and a (C57BL/6 × SP11)F_1 control liver. Duplex PCR was carried out as in Fig. 6A.

than on the maternal chromosome in the brain (55). We found no evidence for differential methylation of this region in ES cells or liver and no evidence for allele-specific differences in H3 acetylation, such as are found at DMR1. However, it is interesting that the paternal DMR2 allele shows relatively increased levels of acetylated H4, comparable to the elevated paternal H4 acetylation seen at DMR1. Allele-specific differences in H4 acetylation at DMR2 clearly do not require differential DNA methylation.

The difference between parental *U2af1-rs1* alleles in levels of H4Ac5, but not of H4Ac8, H4Ac12, or H4Ac16, provides an example in mammalian cells of a lysine-specific acetylation difference associated with a specific function. Previous examples of such associations have been found in *Drosophila* (65) and yeast (6, 51). In *Drosophila*, the preferential acetylation of H4 lysine 16 on the X chromosome in male flies is driven by a histone acetyltransferase with the necessary catalytic specificity (1, 59). The enzymatic basis of the consistent depletion of H4Ac5 on the maternal alleles of the imprinted genes studied here remains to be established, but an H4Ac5-specific deacetylase, targeted to the maternal allele (see below), is a possibility.

Relationship between CpG methylation and histone acetylation. We used a transgenic approach to investigate the relationship between DNA methylation and histone acetylation on the *U2af1-rs1* gene. Full methylation of the paternal *U2af1-rs1* allele can be induced in the male germ line by the presence of multiple copies of a *U2af1-rs1* transgene. Methylation persists in some offspring, even those that lack the transgene itself. For two such nontransgenic offspring with elevated paternal *U2af1-rs1* methylation, we found that the levels of H3 acetylation were extremely low along the paternal *U2af1-rs1* allele (i.e., at the 5′-UTR and 3′-UTR). This result provides in vivo evidence from a mammalian system that CpG methylation can confer hypoacetylation of associated core histones. In contrast to the clear link between DNA methylation and H3 deacetylation, we found no evidence for substantial deacetylation of H4 (at any lysine) in the offspring that had biallelic methylation at *U2af1-rs1*. From this, it seems that whereas CpG methylation, even in an inappropriate chromosomal context, may lead to H3 deacetylation in vivo, it is insufficient, in itself, to bring about deacetylation of H4. The relatively low levels of H4Ac5 on the maternal *U2af1-rs1* allele in all cell types analyzed may be induced by a maternal-chromosome-specific signal other than, or in addition to, CpG methylation. These findings are consistent with the properties of the DMR2 of *Snrpn*, where differential H4 acetylation occurs in the absence of differences in DNA methylation.

MBD proteins and histone deacetylases. Work from several laboratories has provided evidence for the physical association between HDAC1 or HDAC2 and MBD proteins MeCP2 and MBD2 (32, 40, 42, 69). In addition, there are recent data which demonstrate that the methyl-CpG binding protein MBD1 can

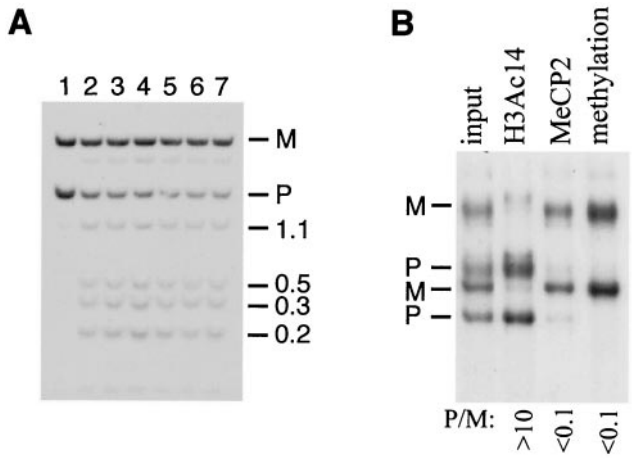

FIG. 8. In vivo association of MeCP2 with the methylated allele of *U2af1-rs1*. (A) *Msp*I sensitivity in nuclei purified from SF1-1 ES cells. Lanes 1 to 7 correspond to 0, 1, 2, 4, 7, 15, and 30 min of incubation with *Msp*I, respectively. Extracted DNA samples were digested with *Bgl*II plus *Sac*I and hybridized with probe 1. Maternal (M) and paternal (P) chromosome-specific bands are indicated, as well as *Msp*I digestion products (in kilobases). (B) Association of MeCP2 with the methylated maternal *U2af1-rs1* allele. SSCP results for the 5'UTR region are shown. PCR amplifications were performed using DNA samples extracted from input native chromatin and from chromatin precipitated with the antisera to H3Ac14 and MeCP2, as indicated. To study allelic methylation (last lane), DNA from input chromatin was digested with *Hpa*II (which has a unique site in the amplified sequences) and amplified with the 5'UTR primers.

also repress methylated genes via histone deacetylation, but here the mechanism seems to involve a deacetylase other than HDAC1 (41). The association of specific MBD proteins with methylated chromosomal DNA would provide an attractive targeting mechanism to account for the observed low acetylation at histones associated with the (methylated) maternal *U2af1-rs1* and *Snrpn* alleles and could also account for the observed H3 hypoacetylation in the nontransgenic offspring with biallelic *U2af1-rs1* methylation. The strong differential sensitivity of the maternal and paternal alleles to digestion with *Msp*I in vivo is revealing. This restriction enzyme recognizes sites that can be methylated, but it is not methylation sensitive. Despite this, the maternal *U2af1-rs1* allele is highly resistant to *Msp*I digestion in embryonic cells and adult liver tissue. One interpretation of these findings is that *Msp*I sensitivity is reduced by proteins that bind specifically to these (CpG-containing) sites on the methylated maternal allele (2). To test this hypothesis, we performed ChIP with antibodies against one of the MBD proteins, MeCP2, on liver chromatin. In vivo association of MeCP2 with *U2af1-rs1* was detected exclusively on the methylated maternal allele.

Collectively, our results support a model in which allele-specific patterns of histone acetylation are regulated, in part, by the targeting of histone deacetylases to the methylated allele. However, whereas the presence of DNA methylation correlates with deacetylation of histone H3 at all lysines tested, it is not sufficient, in itself, to cause deacetylation of H4. Whether this is because of the specificity of the histone deacetylase complexes recruited or because of compensation by selective recruitment of H4-specific HATs remains to be determined. The assays we used detect only steady-state levels of H3 and H4 acetylation at specific regions. They cannot detect differences in turnover, although such differences can be revealed by the use of histone deacetylase inhibitors such as trichostatin A (TSA). It is, however, clear from studies on androgenetic and parthenogenetic ES cells that allele-specific differences in H3 and H4 acetylation generally involve both increased acetylation on the paternal allele (relative to a control, nonimprinted gene) and decreased acetylation on the maternal allele. While targeting of specific MBD proteins seems to play a crucial role in selective histone hypoacetylation, it is unlikely to be the only route by which this is achieved. Further work is needed to determine what other mechanisms could also be involved. For example, recent studies show that specific histone deacetylases can be locally recruited by the maintenance methyltransferase DNMT1 (19, 49).

Differential H3 and H4 acetylation has been found at the 5′ CpG island (DMR1) of the human *SNRPN* gene (52). In this study, reactivation of the repressed maternal allele was associated with an increase in acetylation of H4 but not H3. It seems that on the human *SNRPN* gene, as in the mouse, H3 and H4 acetylation levels are independently regulated. Several recent studies with mice have described allele-specific H4 acetylation at differentially methylated control regions of the imprinted *Igf2r* and *H19* loci (22, 30). As at *Snrpn* and *U2af1-rs1*, acetylation at these germ line DMRs is consistently low on the methylated allele. In attempts to determine the role of allele-specific histone acetylation in the regulation of imprinted-gene expression, several recent studies have examined the effects of growing cultured cells in the presence of the histone deacetylase inhibitor TSA. In some cases, this leads to transient induction of gene expression from the normally silent allele. Such effects have been demonstrated for *Igf2, Igf2r*, and *p57Kip2* (3, 16, 22, 30). However, expression of other imprinted genes, including *Snrpn* and *U2af1-rs1*, appears to remain unaltered on exposure to TSA (16, 52). We also did not observe changes in the allelic expression of *U2af1-rs1* or *Snrpn* on culture of ES and differentiated cells in the presence of TSA, although TSA treatment did induce changes in chromatin conformation at *U2af1-rs1* (R. I. Gregory, S. Khosla, and R. Feil, unpublished results). Maintenance of the allele-specific differences in the expression of imprinted genes requires several interacting components, including DNA methylation, MBD proteins, histone deacetylases, and histone acetylation. Methylation-dependent targeting of histone deacetylases via MBD proteins such as MeCP2 is likely to be an important mechanism for setting levels of H3 acetylation, but other, methylation-independent mechanisms are likely to also be involved, at least for histone H4.

ACKNOWLEDGMENTS

We thank Wolf Reik, Peter Fraser, and Gavin Kelsey for critical reading of the manuscript.

This work was supported by the Biotechnology and Biological Sciences Research Council (Studentship to R.I.G.), the Wellcome Trust (grant 045030/Z/95 to B.M.T.), the Human Frontier Science Program (grant RG0083/1999 to R.F., I.H., and Neil Brockdorff), the Centre National de la Recherche Scientifique (ATIPE grant to R.F.), the Fondation pour la Recherche Médicale (to R.F.), and the Royal Society (Fellowship 516002 to L.P.O.).

REFERENCES

1. **Akhtar, A., and P. B. Becker.** 2000. Activation of transcription through H4 acetylation by MOF, an acetyltransferase essential for dosage compensation in *Drosophila*. Mol. Cell **5:**367–375.
2. **Antequera, F., J. Boyes, and A. Bird.** 1990. High levels of de novo methylation and altered chromatin structure at CpG islands in cell lines. Cell **62:**503–514.
3. **Bestor, T. H.** 2000. The DNA methyltransferases in mammals. Hum. Mol. Genet. **12:**2395–2402.
4. **Bielinska, B, S. M. Blaydes, K. Buiting, T. Yang, M. Krajewska-Walasek, B. Horsthemke, and C. I. Brannan.** 2000. *De novo* deletions of *SNRPN* exon 1 in early human and mouse embryos result in a paternal to maternal imprint switch. Nat. Genet. **25:**74–78.
5. **Bird, A. P., and A. P. Wolffe.** 1999. Methylation-induced repression—belts, braces, and chromatin. Cell **99:**451–454.
6. **Braunstein, M., R. E. Sobel, C. D. Allis, B. M. Turner, and J. R. Broach.** 1996. Efficient transcriptional silencing in *Saccharomyces cerevisiae* requires a heterochromatin histone acetylation pattern. Mol. Cell. Biol. **16:**4349–4356.
7. **Caspary, T, M. A. Cleary, C. C. Baker, X. J. Guan, and S. M. Tilghman.** 1998. Multiple mechanisms regulate imprinting of the mouse distal chromosome 7 cluster. Mol. Cell. Biol. **18:**3466–3474.
8. **Cavalli, G., and R. Paro.** 1999. Epigenetic inheritance of active chromatin after removal of the main transactivator. Science **286:**955–958.
9. **Chen, H., R. J. Lin, W. Xie, D. Wilpitz, and R. M. Evans.** 1999. Regulation of hormone-induced histone hyperacetylation and gene activation via acetylation of an acetylase. Cell **98:**675–686.
10. **Cheung, P., K. G. Tanner, W. L. Cheung, P. Sassone-Corsi, J. M. Denu, and C. D. Allis.** 2000. Synergistic coupling of histone H3 phosphorylation and acetylation in response to epidermal growth factor stimulation. Mol. Cell **5:**905–915.
11. **Clayton, A. L., S. Rose, M. J. Barratt, and L. C. Mahadevan.** 2000. Phosphoacetylation of histone H3 on c-fos- and c-jun-associated nucleosomes upon gene activation. EMBO J. **19:**3714–3726.
12. **Constância, M., B. Pickard, G. Kelsey, and W. Reik.** 1998. Imprinting mechanisms. Genome Res. **8:**881–900.
13. **Dean, W. L., L. Bowden, A. Aitchison, J. Klose, T. Moore, J. J. Meneses, W. Reik, and R. Feil.** 1998. Altered imprinted gene methylation and expression in completely ES cell-derived mouse fetuses: association with aberrant phenotypes. Development **125:**2273–2282.
14. **Drewell, R. A., J. D. Brenton, J. F. Ainscough, S. C. Barton, K. Hilton, K. L. Arney, L. Dandolo, and M. A. Surani.** 2000. Deletion of a silencer element disrupts *H19* imprinting independently of a methylation epigenetic switch. Development **127:**3419–3428.
15. **Ekwall K., T. Olsson, B. M. Turner, G. Cranston, and R. C. Allshire.** 1997. Transient inhibition of histone deacetylation alters the structural and functional imprint at fission yeast centromeres. Cell **91:**1021–1032.
16. **El Kharroubi, A., G. Piras, and C. L. Stewart.** 2001. DNA demethylation reactivates a subset of imprinted genes in uniparental mouse embryonic fibroblasts. J. Biol. Chem. **276:**8674–8680.
17. **Feil, R., M. D. Boyano, N. D. Allen, and G. Kelsey.** 1997. Parental chromosome-specific chromatin conformation in the imprinted *U2af1-rs1* gene in the mouse. J. Biol. Chem. **272:**20893–20900.
18. **Feil, R., and S. Khosla.** 1999. Genomic imprinting in mammals: an interplay between chromatin and DNA methylation? Trends Genet. **15:**431–435.
19. **Fuks, F., W. A. Burgers, A. Brehm, L. Hughes-Davies, and T. Kouzarides.** 2000. DNA methyltransferase Dnmt1 associates with histone deacetylase activity. Nat. Genet. **24:**88–91.
20. **Gerelli, D., N. G. Sharpe, and D. S. Latchman.** 1991. Cloning and sequencing of a mouse embryonal carcinoma cell mRNA encoding the tissue specific RNA splicing factor SmN. Nucleic Acids Res. **19:**6642.
21. **Glenn, C. C., S. Saitoh, M. T. Jong, M. M. Filbrandt, U. Surti, D. J. Driscoll, and R. D. Nicholls.** 1996. Gene structure, DNA methylation, and imprinted expression of the human *SNRPN* gene. Am. J. Hum. Genet. **58:**335–346.
22. **Grandjean, V., L. O'Neill, T. Sado, B. Turner, and A. Ferguson-Smith.** 2001. Relationship between DNA methylation, histone H4 acetylation and gene expression in the mouse imprinted *Igf2–H19* domain. FEBS Lett. **488:**165–169.
23. **Gregory, R. I., and R. Feil.** 1999. Analysis of chromatin in limited numbers of cells: a PCR-SSCP based assay of allele-specific nuclease sensitivity. Nucleic Acids Res. **27:**R1–R4.
24. **Grunstein M.** 1998. Inheritance by histones. Cell **93:**325–328.
25. **Hansen, J. C., C. Tse, and A. P. Wolffe.** 1998 Structure and function of the core histone N-termini: more than meets the eye. Biochemistry **37:**17637–17641.
26. **Hatada, I., A. Nabetani, Y. Arai, S. Ohishi, M. Suzuki, S. Miyabara, Y. Nishimune, and T. Mukai.** 1997. Aberrant methylation of an imprinted gene *U2af1-rs1* (SP2) caused by its own transgene. J. Biol. Chem. **272:**9120–9122.
27. **Hatada, I., T. Sugama, and T. Mukai.** 1993. A new imprinted gene cloned by a methylation-sensitive genome scanning method. Nucleic Acids Res. **21:**5577–5582.
28. **Hayashizaki, Y., H. Shibata, S. Hirotsune, H. Sugino, Y Okazaki, N. Sasaki, K. Hirose, H. Imoto, H. Okuizumi, M. Muramatsu, H. Komatsubara, T. Shiroishi, K. Moriwaki, M. Katsuki, N. Hatano, H. Sasaki, T. Ueda, N. Mise, N. Takagi, C. Plass, and V. M. Chapman.** 1994. Identification of an imprinted U2af binding protein related sequence on mouse chromosome 11 using the RLGS method. Nat. Genet. **6:**33–39.
29. **Hebbes, T. R., A. L. Clayton, A. W. Thorne and C. Crane-Robinson.** 1994. Core histone hyperacetylation co-maps with generalised DNaseI sensitivity in the chicken β-globin chromosomal domain. EMBO J. **13:**1823–1830.
30. **Hu, J.-F., J. Pham, I. Dey, T. Li, T. H. Vu, and A. R. Hoffman.** 2000. Allele-specific histone acetylation accompanies genomic imprinting of the insulin-like growth factor II receptor gene. Endocrinology **141:**4428–4435.
31. **Johnson, C. A., L.P. O'Neill, A. Mitchell, and B. M. Turner.** 1998 Distinctive patterns of histone H4 acetylation are associated with defined sequence elements within both heterochromatic and euchromatic regions of the human genome. Nucleic Acids Res. **26:**994–1001.
32. **Jones, P. L., G. J. Veenstra, P. A. Wade, D. Vermaak, S. U. Kass, N. Landsberger, J. Strouboulis, and A. P. Wolffe.** 1998. Methylated DNA and MeCP2 recruit histone deacetylase to repress transcription. Nat. Genet. **19:**187–191.
33. **Kafri, T., M. Ariel, M. Brandeis, R. Shemer, L. Urven, J. McCarrey, H. Cedar, and A. Razin.** 1992. Developmental pattern of gene-specific DNA methylation in the mouse embryo and germ line. Genes Dev. **6:**705–714.
34. **Kuo, M. H., J. Zhou, P. Jambeck, M. E. A. Churchill, and C. D. Allis.** 1998. Histone acetyltransferase activity of yeast Gcn5p is required for the activation of target genes in vivo. Genes Dev. **12:**627–639.
35. **Leff, S. E., C. I. Brannan, M. L. Reed, T. Ozcelik, U. Francke, N. G. Copeland, and N. A. Jenkins.** 1992. Maternal imprinting of the mouse *Snrpn* gene and conserved linkage homology with the human Prader-Willi syndrome region. Nat. Genet. **2:**259–264.
36. **Li, E., C. Beard, and R. Jaenisch.** 1993. Role of DNA methylation in genomic imprinting. Nature **366:**362–365.
37. **Luger, K., and T. J. Richmond.** 1998. Histone tails of the nucleosome. Curr. Opin. Genet. Dev. **8:**140–146.
38. **Lyko, F., and R. Paro.** 1999. Chromosomal elements conferring epigenetic inheritance. Bioessays **21:**824–832.
39. **Mayer, W., A. Niveleau, J. Walter, R. Fundele, and T. Haaf.** 2000. Demethylation of the zygotic paternal genome. Nature **403:**501–502.
40. **Nan, X., H.-H. Ng, C. A. Johnson, C. D. Laherty, B. M. Turner, R. N. Eisenman, and A. Bird.** 1998. Transcriptional repression by the methyl CpG binding protein MeCP2 involves a histone acetylase complex. Nature **393:**386–389.
41. **Ng, H.-H., P. Jeppesen, and A. Bird.** 2000. Active repression of methylated genes by the chromosomal protein MBD1. Mol. Cell. Biol. **20:**1394–1406.
42. **Ng, H.-H., Y. Zhang, B. Hendrich, C. A. Johnson, B. M. Turner, H. Erdjument-Bromage, P. Tempst, D. Reinberg, and A. Bird.** 1999. MBD2 is a transcriptional repressor belonging to the MeCP1 histone deacetylase complex. Nat. Genet. **23:**58–61.
43. **O'Neill, L. P., A. M. Keohane, J. S. Lavender, V. McCabe, E. Heard, P. Avner, N. Brockdorff, and B. M. Turner.** 1999. A developmental switch in H4 acetylation upstream of *Xist* plays a role in X chromosome inactivation. EMBO J. **18:**2897–2907.
44. **O'Neill, L. P., and B. M. Turner.** 1995. Histone H4 acetylation distinguishes coding regions of the human genome from heterochromatin in a differentiation-independent manner. EMBO J. **14:**3946–3957.
45. **Parekh, B. S., and T. Maniatis.** 1999. Virus infection leads to localized hyperacetylation of histones H3 and H4 at the IFN-β promoter. Mol. Cell **3:**125–129.
46. **Pfeifer, K.** 2000. Mechanisms of genomic imprinting. Am J. Hum. Genet. **67:**777–787.
47. **Rea, S., F. Eisenhaber, D. O'Carroll, B. D. Strahl, Z. W. Sun, M. Schmid, S. Opravil, K. Mechter, C. P. Ponting, C. D. Allis, and T. Jenuwein.** 2000. Regulation of chromatin structure by site-specific histone H3 methyltransferases. Nature **406:**593–599.
48. **Reik, W., and J. Walter.** 1998. Imprinting mechanisms in mammals. Curr. Opin. Genet. Dev. **8:**154–164.
49. **Robertson, K. D., S. Ait-Si-Ali, T. Yokochi, P. A. Wade, P. L. Jones, and A. P. Wolffe.** 2000. DNMT1 forms a complex with Rb, E2F1 and HDAC1 and represses transcription from E2F-responsive promoters. Nat. Genet. **25:**338–342.
50. **Rougier, N., D. Bourc'his, D. M. Gomes, A. Niveleau, M. Planchot, A. Paldi, and E. Viegas-Pequignot.** 1998. Chromosome methylation patterns during mammalian preimplantation development. Genes Dev. **12:**2108–2113.
51. **Rundlett, S. E., A. A. Carmen, N. Suka, B. M. Turner, and M. Grunstein.** 1998. Transcriptional repression by UME6 involves deacetylation of lysine 5 of histone H4 by RPD3. Nature **392:**831–835.
52. **Saitoh, S., and T. Wada.** 2000. Parent-of-origin specific histone acetylation and reactivation of a key imprinted gene locus in Prader-Willi syndrome. Am. J. Hum. Genet. **66:**1958–1962.
53. **Schübeler D., C. Francastel, D. M. Cimbora, A. Reik, D. I. Martin, and M. Groudine.** 2000. Nuclear localization and histone acetylation: a pathway for

chromatin opening and transcriptional activation of the human beta-globin locus. Genes Dev. **14:**940–950.
54. **Shemer, R., A. Y. Hersko, J. Perk, R. Mostoslavsky, B. Z. Tsuberi, H. Cedar, K. Buiting, and A. Razin.** 2000. The imprinting box of the Prader-Willi/Angelman syndrome domain. Nat. Genet. **26:**440–443.
55. **Shemer, R., Y. Birger, A. D. Riggs, and A. Razin.** 1997. Structure of the imprinted mouse *Snrpn* gene and establishment of its parental-specific methylation pattern. Proc. Natl. Acad. Sci. USA **94:**10267–10272.
56. **Shibata, H., K. Yoshino, S. Sunahara, Y. Gondo, M. Katsuki, T. Ueda, M. Kamiya, M. Muramatsu, Y. Murakami, L. Kalcheva, C. Plass, V. N. Chapman, and Y. Hayashizaki.** 1996. Inactive allele-specific methylation and chromatin structure of the imprinted gene *U2af1-rs1* on mouse chromosome 11. Genomics **35:**248–252.
57. **Shibata, H., T. Ueda, M. Kamiya, A. Yoshida, M. Kusakabe, C. Plass, W. A. Held, S. Sunahara, M. Katsuki, M. Muramatsu, and Y. Hayashizaki.** 1997. An oocyte-specific methylation imprint center in the mouse *U2afbp-rs*/*U2af1-rs1* gene marks the establishment of allele-specific methylation during preimplantation development. Genomics **44:**171–178.
58. **Sleutels, F., D. P. Barlow, and R. Lyle.** 2000. The uniqueness of the imprinting mechanism. Curr. Opin. Genet. Dev. **10:**229–233.
59. **Smith, E. R., A. Pannutti, W. Gu, A. Steurnagel, R. G. Cook, C. D. Allis, and J. C. Lucchesi.** 2000. The *Drosophila* MSL complex acetylates histone H4 at lysine 16, a chromatin modification linked to dosage compensation. Mol. Cell. Biol. **20:**312–318.
60. **Strahl, B. D., R. Ohba, R. G. Cook, and C. D. Allis.** 1999. Methylation of histone H3 at lysine 4 is highly conserved and correlates with transcriptionally active nuclei in *Tetrahymena*. Proc. Natl. Acad. Sci. USA **96:**14967–14972.
61. **Strahl, B. D., and C. D. Allis.** 2000. The language of covalent histone modifications. Nature **403:**41–45.
62. **Tanaka, M., M. Puchyr, M. Gerstenstein, K. Harpal, R. Jaenisch, J. Rossant, and A. Nagy.** 1999. Parental origin-specific expression of *Mash2* is established at the time of implantation with its imprinting mechanism highly resistant to genome-wide demethylation. Mech. Dev. **87:**129–142.
63. **Turner, B. M.** 1998. Histone acetylation as an epigenetic determinant of long-term transcriptional competence. Cell. Mol. Life Sci. **54:**21–31.
64. **Turner, B. M.** 2000. Histone acetylation and an epigenetic code. Bioessays **22:**836–845.
65. **Turner, B. M., A. J. Birley, and J. Lavender.** 1992. Histone H4 isoforms acetylated at specific lysine residues define individual chromosomes and chromatin domains in *Drosophila* polytene nuclei. Cell **69:**375–384.
66. **Turner, B. M., and G. Fellows.** 1989. Specific antibodies reveal ordered and cell-cycle-related use of histone-H4 acetylation sites in mammalian cells. Eur. J. Biochem. **179:**131–139.
67. **White, D. A., N. D. Belyaev, and B. M. Turner.** 1999. Preparation of site-specific antibodies to acetylated histones. Methods **19:**417–424.
68. **Wolffe, A. P.** 2000. Transcriptional control: imprinting insulation. Curr. Biol. **10:**R463–R465.
69. **Zhang, Y., H.-H. Ng, H. Erdjument-Bromage, P. Tempst, A. Bird, and D. Reinberg.** 1999. Analysis of the NuRD subunits reveals a histone deacetylase core complex and a connection with DNA methylation. Genes Dev. **13:**1924–1935.